# A chalcone derivative suppresses the induction of TSLP in mice and human keratinocytes and attenuates OVA-induced antibody production in mice



doi: 10.1016/j.ejphar.2019.02.007

# A chalcone derivative suppresses the induction of TSLP in mice and human keratinocytes and attenuates OVA-induced antibody production in mice

Ryosuke Segawa[a], Mika Shiraki[a], Shiori Sudo[a], Kenichi Shigeeda[a], Taiji Saito[a], Natsumi Mizuno[a], Takahiro Moriya[a, b], Takayuki Yonezawa[c], Je-Tae Woo[d], Masahiro Hiratsuka[a], Noriyasu Hirasawa[a,*]

[a]Laboratory of Pharmacotherapy of Life-Style Related Diseases, Graduate School of Pharmaceutical Sciences, Tohoku University, Sendai 980-8578, Miyagi, Japan

[b]Department of Pharmacology, School of Pharmaceutical Sciences, Ohu University, Koriyama 963-8611, Fukushima, Japan.

[c]Research Institute for Biological Functions, Chubu University, Kasugai 487-8501, Aichi, Japan

[d]Department of Biological Chemistry, College of Bioscience and Biotechnology, Chubu University, Kasugai 487-8501, Aichi, Japan

*Corresponding author at: Laboratory of Pharmacotherapy of Life-Style Related Diseases, Graduate School of Pharmaceutical Sciences, Tohoku University, Sendai 980-8578, Miyagi, Japan.

Phone: +81-22-795-6809

Fax: +81-22-795-3847

E-Mail: hirasawa@m.tohoku.ac.jp

**Abstract**

Thymic stromal lymphopoietin (TSLP) is a key epithelial-derived factor that aggravates allergic diseases. Therefore, TSLP inhibitors are candidate compounds for the treatment of allergic diseases. Previously, we reported that KCMH-1, a mouse keratinocyte cell line, constitutively produces TSLP. In this study, we tried to identify inhibitors of TSLP by screening 2169 compounds in KCMH-1 cells and found one such chalcone derivative (code no. 16D10). 16D10 inhibited TSLP expression and TSLP promoter activation in HaCaT cells, a human keratinocyte cell line. Although nuclear factor kappa-B (NF-κB) is a key transcription factor for the induction of TSLP, 16D10 did not inhibit the activation pathway of NF-κB, such as degradation of inhibitor of κB (IκB) and p65 nuclear translocation. 16D10 activated the Kelch-like ECH-associated protein 1 (Keap1)-nuclear factor (erythroid-derived 2)-like 2 (Nrf2) system, although this system was not involved in the inhibitory effect of 16D10. 16D10 also inhibited TSLP production in a lipopolysaccharide (LPS)- or ovalbumin (OVA)-induced air-pouch-type inflammation model. Further, repeated 16D10 administration diminished serum immunoglobulin G1 (IgG1) and IgE concentration in an OVA-induced air-pouch-type sensitization model. Taken together, these results indicate that 16D10 is an inhibitor of TSLP production and has an anti-allergic effect. This inhibitory effect is independent of the activation of NF-κB and the Keap1-Nrf2 system. Therefore, 16D10 could be a new type of candidate drug for allergic diseases.

**Key words:** Allergy, thymic stromal lymphopoietin, keratinocyte, 16D10, chalcone, air-pouch-type inflammation

## 1. Introduction

Atopic dermatitis is one of the most common diseases. The hallmarks of atopic dermatitis are relapsing skin inflammation, itch, epithelial barrier dysfunction, and high levels of serum immunoglobulin E (IgE) antibody. Excessive T helper cell type 2 (Th2)-type immune reactions relate to these symptoms. The number of patients with atopic dermatitis has increased in the past few decades in both developed and developing countries (Weidinger and Novak, 2016). Atopic dermatitis affects various factors of health-related quality of life such as work productivity and activity (Eckert et al., 2018). In addition, atopic dermatitis is a risk factor for other allergic diseases and leads the atopic march (Lowe et al., 2018). Therefore, overcoming atopic dermatitis is an important issue worldwide.

Although there are many medicines available for the symptoms of atopic dermatitis, treatment and prevention strategies are not fully established. Topical corticosteroids and immunosuppressive agents are the major medications used for the treatment of atopic dermatitis. The efficacy of these medications has been reported by many randomized clinical trials (Ashcroft, 2005; Hoare et al., 2000). However, glucocorticoids have many side effects, such as increasing susceptibility to infection and induction of skin atrophy, in infants and long-term users (Boguniewicz et al., 2017). Immunosuppressive agents such as tacrolimus have fewer side effects but have usage dose limitations (Siegfried et al., 2016). In addition, these medications do not prevent the onset of atopic dermatitis. Therefore, new targets for treatment and prevention are required.

Thymic stromal lymphopoietin (TSLP) has been reported as a treatment target for atopic dermatitis. TSLP is an epithelial cell-derived cytokine that plays critical roles in

immune regulation in the skin (Omori-Miyake and Ziegler, 2012). TSLP is highly expressed in the epithelia of patients with atopic dermatitis (Soumelis et al., 2002) and activates various immune cells, such as dendritic cells, T cells, mast cells and basophils (Salter et al., 2015; Tatsuno et al., 2015; Ziegler and Artis, 2010). TSLP-activated immune cells produce Th2 cytokines and chemokines (Allakhverdi et al., 2007; He et al., 2008), and promote Th2-type immune reactions. A deficiency in TSLP receptors reduced allergic skin inflammation in ovalbumin (OVA)-sensitized mice (He et al., 2008). Recently, it was shown that human anti-TSLP monoclonal immunoglobulin treatment attenuated allergen-induced asthmatic responses in patients with mild allergic asthma (Gauvreau et al., 2014). In a meta-analysis of genome-wide association studies (GWAS) of atopic dermatitis or asthma patients, the single nucleotide polymorphism of TSLP, rs1837253, was associated with increased susceptibility for these diseases (Jiang et al., 2017; Torgerson et al., 2011). In addition, skin TSLP promotes allergic airway inflammation and leads the atopic march (Jiang et al., 2012; Lowe et al., 2018). Hence, skin-derived TSLP strongly contributes to the pathogenesis of allergic diseases and is a molecular target for the treatment of these diseases.

Recently, we reported that KCMH-1, a mouse keratinocyte cell line, constitutively and highly produced functional TSLP (Segawa et al., 2014). In the current study, we tried to identify inhibitors of TSLP production by Screening a chemical compounds library in KCMH-1 cells, and identified one positive chalcone-structure compound, N-[2-[2-[(2E)-3-(2,5-dimethoxyphenyl)-1-oxo-2-propen-1-yl]-4,5-dimethoxyphenyl]ethyl]acetamide, with code no. 16D10. We also investigated the effect of 16D10 on TSLP production *in vitro* and *in vivo* and on antibody production in an OVA allergen sensitization murine model.

## 2. Materials and Methods

### *2.1 Materials*

The chemical library was obtained from InterBioScreen LTD. (Moscow, Russia) and 16D10 from Hamari Chemicals, Ltd (Osaka, Japan). STK381202, (2E)-3-(2,5-dimethoxyphenyl)-1-(3,4-dimethoxyphenyl)-2-Propen-1-one, was purchased from Vitas-M Laboratory (Moscow, Russia), 2,5-dimethoxy cinnamic acid from Wako Pure Chemical Ind (Osaka, Japan) and SI37006, N-[2-(3,4-dimethoxyphenyl)ethyl]acetamide, from Sigma-Aldrich (St. Louis, MO). Diethyl maleate (DEM), lipopolysaccharide (LPS) were obtained from Wako Pure Chemical Ind. Dulbecco's modified Eagle's medium (DMEM) was purchased from Nissui Pharmaceutical Co (Tokyo, Japan) and alpha minimal essential medium (MEM-α) from Life Technologies (Grand Island, NY, USA). The Keratinocyte Growth Medium (KGM)-Gold Bullet Kit was purchased from Lonza (Walkersville, MD). Fetal bovine serum (FBS) was obtained from Biowest (Miami, FL) and penicillin G potassium and streptomycin sulfate from Meiji Seika Co (Tokyo, Japan). Human recombinant tumor necrosis factor alpha (TNF-α) was purchased from Peprotech (Rocky Hill, NJ). The inhibitor of nuclear factor kappa-B kinase 2 (IKK-2) inhibitor, TPCA-1, was obtained from Cayman Chemical Co. (Ann Arbor, MI). Thiazolyl blue tetrazolium bromide (MTT) was purchased from Sigma Aldrich Co. (St Louis, MO, USA). Antibodies against inhibitor of κB alpha (IκB-α) and nuclear factor (erythroid-derived 2)-like 2 (Nrf2) were obtained from Cell Signaling Technology (Beverly, MA). Anti-α-tubulin, actin, and p65 antibodies were purchased from Santa Cruz Biotechnology. Horseradish peroxidase (HRP)-linked anti-mouse and anti-rabbit

IgG were obtained from Cell Signaling Technology (Beverly, MA). Biotinylated anti-goat and anti-rabbit IgG antibodies were purchased from Vector Laboratories (Burlingame, CA). Rabbit IgG (H+L) Cross-Adsorbed Secondary Antibody, Alexa Fluor 488 (A-11070) was obtained from Thermo Fisher Scientific (Melbourne, Australia). Goat-anti mouse IgE was obtained from Southern Biotech (Birmingham, AL). Biotin-labeled OVA was purchased from Nanocs Inc. (New York, NY, USA). Anti-OVA IgE (mouse) ELISA standard was bought from Cayman Chemical Co. (Ann Arbor, MI). TMB Microwell Peroxidase Substrate was obtained from SeraCare Life Sciences, Inc. (Milford, MA, USA). The Vectastain Elite ABC Peroxidase staining kit (standard) was purchased from Vector Laboratories. OVA and BSA were bought from Sigma-Aldrich (St. Louis, MO). 4',6-diamidino-2-phenylindole (DAPI) was purchased from Dojindo Laboratories (Kumamoto, Japan). Nrf2 and Keap1 MISSION endoribonuclease-prepared small interfering RNA (esiRNA) were obtained from Sigma-Aldrich (St. Louis, MO). Lipofectamine RNAiMAX Transfection Reagent and Opti-MEM were purchased from Thermo Fisher Scientific (Waltham, MA).

*2.2 Animals*

Male BALB/c and ICR mice (5-7 weeks old) were purchased from SLC (Shizuoka, Japan). These mice were housed in standardized specific pathogen-free conditions. All animal experiments were approved by the Animal Ethics Committee of Tohoku University.

*2.3 Cell culture*

KCMH-1 is a mouse keratinocyte cell line that produces constitutively high levels of

TSLP (Segawa et al., 2014). The cells were cultured in MEM-α supplemented with 10% FBS, 18 μg/ml of penicillin G potassium, and 50 μg/ml streptomycin sulfate, and maintained at 37°C, 5% $CO_2$, and 95% relative humidity. The cells were seeded at $1 \times 10^5$ cells/ml in multi-well plates for the experiments. HaCaT cells were maintained in DMEM supplemented with 10% FBS, 18 μg/ml of penicillin G potassium, and 50 μg/ml streptomycin sulfate, and maintained at 37°C, 5% $CO_2$, and 95% relative humidity. In the experiments using HaCaT cells, the KGM-Gold Bullet Kit was used. HaCaT cells were seeded at a density of $0.5\text{-}1 \times 10^5$ cells/ml in complete KGM medium (GA-1000, epinephrine, transferrin, insulin, bovine pituitary extract, hydrocortisone, and hEGF added) and incubated for 2 days. After this, the medium was replaced with the same volume of incomplete KGM medium (no bovine pituitary extract, hydrocortisone, and hEGF added), and incubated for 24 h. After 24 h, HaCaT cells were treated with TNF-α and polyinosinic-polycytidylic acid (poly(I:C)) with or without 16D10.

*2.4 MTT assay*

MTT was dissolved in PBS to a concentration of 5 mg/ml. After the treatment of KCMH-1 cells with chemical compounds for 24 h, MTT solution was added to the culture medium to a final concentration of 0.5 mg/ml. After incubation for another 2-4 h, formazan crystals in the cells were dissolved in DMSO, and absorbance was measured at 595 nm using the iMark Microplate Absorbance Reader (Bio-Rad, Hercules, CA).

*2.5 Measurement of cytokines and OVA-specific antibodies concentration*

TSLP, interleukin (IL)-1β, and TNFα levels in the pouch fluids and the supernatants of KCMH-1 cells were determined by specific ELISAs (mouse and human TSLP and human IL1β ELISA: R&D Systems, Minneapolis, MN, USA; human TNF-α ELISA: eBioscience, San Diego, CA, USA). Mouse serum OVA-specific IgG1 concentration was determined using Anti-Ovalbumin IgG1 Antibody EIA Kit (Cayman Chemical Co., Ann Arbor, MI). The ELISAs were performed according to the manufacturer's protocols. Mouse serum OVA-specific IgE concentration was determined as follows. Each well in the 96-well plates were coated with 100 μl of 2 μg/ml goat-anti mouse IgE, washed four times with 300 μl of 0.05% Tween-20-PBS, and then treated with 1% BSA-PBS for 1 h. After blocking, the wells were washed once and 100 μl of diluted serum samples or standards were added, and the plate was incubated at room temperature for 2 h. After 2 h incubation, these were washed four times, 100 μl of 1 μg/ml biotin-labeled OVA was added, and the plate was incubated at room temperature for 1 h. After 1 h incubation, the wells were washed four times, and 100 μl of streptavidin-HRP solution was added, before incubating at room temperature for 30 min. After 30 min incubation, the wells were washed four times, and 100 μl of TMB substrate was added. The plate was incubated at room temperature for a further 20 min. After 20 min incubation, the reaction was stopped by adding 50 μl of 1 M $H_3PO_4$ solution and the absorbance was measured at 450 nm.

*2.6 TSLP inhibitor screening*

KCMH-1 cells were seeded at a density of $1 \times 10^4$ cells/well in 96-well plates and incubated for 24 h. Then, the cells were treated with 30 μg/ml of each chemical compounds in the library (2169 compounds, InterBioScreen LTD., Moscow, Russia) for

a further 24 h. The mouse TSLP ELISA and MTT assay were performed using the supernatants. Chemical compounds that suppressed TSLP production to ≤ 25% of that in the control were considered primary hit compounds. The concentration-dependent effects of primary hit compounds (3, 10, and 30 μg/ml) on TSLP production and viability were assessed by TSLP ELISA and MTT assay as described above.

*2.7 RNA extraction, reverse transcription and quantitative real-time PCR (RT-qPCR)*

KCMH-1 or HaCaT cells were washed with ice-cold PBS and lysed using RNAiso Plus (TaKaRa, Shiga, Japan). Total RNA was isolated according to the manufacturer's protocol for RNAiso Plus. Reverse transcription was performed using a PrimeScript RT Master Mix (TaKaRa, Shiga, Japan). PCR for the specific genes was conducted using SYBR® Premix Ex Taq™ II (Tli RNaseH Plus) (TaKaRa, Shiga, Japan). Complementary DNA sequences (cDNA, 10-30 ng) were amplified using the following primers: mouse *Gapdh*, 5′-TGTGTCCGTCGTGGATCTTA-3′ (forward) and 5′-TTGCTGTTGAAGTCGCAGGAG-3′ (reverse); mouse *Tslp*, 5′-AGCTTGTCTCCTGAAAATCGAG-3′ (forward) and 5′-AGGTTTGATTCAGGCAGATGTT-3′ (reverse); human *GAPDH*, 5′-GAGTCAACGGATTTGGTCGT-3′ (forward) and 5′-CATGGGTGGAATCATATTGGA-3′ (reverse); human *TSLP*, 5′-GATTACATATATGAGTGGGAC-3′ (forward) and 5′-TTCATTGCCTGAGTAGCAT-3′ (reverse); human *HMOX-1*, 5′-TAGAAGAGGCCAAGACTGCG-3′ (forward) and 5′-TCCTTGGTGTCATGGGTCAG-3′ (reverse). Relative quantities of target mRNAs were determined using the comparative CT method (ΔΔCT method). Primer

specificities were confirmed via melting curve analysis. Mouse *Gapdh* and human *GAPDH* were used as normalization controls. When making primers for human *TSLP*, we referred to the sequence of *Homo sapiens* thymic stromal lymphopoietin transcript variant 1, named long-form TSLP.

*2.8 Luciferase assay*

The TSLP promoter reporter plasmid was kindly provided by Dr. Tamari, Institute of Physical and Chemical Research, Japan (Harada et al., 2009). The thymidine kinase (TK) and cytomegalovirus (CMV) reporter plasmid were purchased from Promega (Madison, WI). For deletion of TSLP promoter region, a KOD -plus- Mutagenesis Kit (Toyobo, Tokyo, Japan) was used. Primers for this deletion are as follows; 5′-GCCCTGTAGGAGAAAGACACTGGTATC-3′ (forward) and 5′-TATCGATAGAGAAATGTTCTGGCACCTGC-3′ (reverse). KCMH-1 cells were seeded at a density of $0.5 \times 10^5$ cells/well in 24-well plates and incubated for 24 h. Then, KCMH-1 cells were transfected with the TSLP promoter reporter or the NF-κB reporter plasmid (250 ng in each well) and CMV reporter plasmid (10 ng in each well) for 12 h. X-tremeGENE HP DNA Transfection Reagent (Roche, Basel, Switzerland) was used for plasmid transfection. The cells were then treated with 16D10 (1, 3, and 10 μM), and TPCA-1 (3 μM) for 12 h. The Dual-luciferase reporter assay system (Promega, WI) was used for the measurement of *Firefly* and *Renilla* luciferase activity. The measurements were conducted according to the manufacturer's protocols. HaCaT cells were seeded in KGM medium at a density of $0.35\text{-}0.5 \times 10^5$ cells/well in 24-well plates. Two days later, medium was exchanged for incomplete KGM medium and cells were transfected with TSLP promoter reporter plasmid (250 ng in each well) and

TK reporter plasmid (100 ng in each well) or CMV reporter plasmid (10 ng in each well) for 24 h. The cells were then stimulated with TNF-α (100 ng/ml) with or without 16D10 (10 μM) for 2 h. Measurement of luciferase activity was conducted as described above.

*2.9 Western blotting*

HaCaT cells were washed twice with ice-cold PBS and lysed with ice-cold lysis buffer (20 mM HEPES buffer including 1% (v/v) Triton X-100, 10% (v/v) glycerol, 1 mM EDTA, 50 mM sodium fluoride, 2.5 mM p-nitrophenyl phosphate, 10 μg/ml phenylmethylsulfonyl fluoride, 1mM Na3VO4, and 10 μg/ml leupeptin). Cell lysates were denatured and subjected to 10% (w/v) SDS-PAGE. Proteins were transferred onto nitrocellulose membranes (GE Healthcare, Buckinghamshire, England), and the membranes were blocked using 4% (w/v) Block Ace (Dainippon Pharmaceutical Co., Japan) in deionized water. Membranes were washed with TTBS (40 mM Tris, 300 mM NaCl, 0.1% (v/v) Tween 20, pH 7.5) and incubated overnight at 4°C with antibodies. Membranes were washed with TTBS six times for 5 min each, and then incubated with biotinylated anti-goat and anti-rabbit IgG antibodies or HRP-conjugated anti-mouse and anti-rabbit IgG antibodies for 1.5 to 3 h. After incubation with biotinylated antibodies, membranes were washed with TTBS six times for 5 min each and incubated with avidin-biotin complex solution for 30 min at room temperature. Before detection, membranes were washed with TTBS as previously. After washing, the immunoreactive bands were detected using a chemiluminescence detection system (ECL system, PerkinElmer Life Sciences, Boston, MA).

*2.10 Immunostaining for p65*

HaCaT cells were seeded in KGM medium at a density of $0.5 \times 10^5$ cells/well in a Glass Base Dish (IWAKI, Japan). Two days later, medium was exchanged for incomplete KGM medium and the cells were incubated for 24 h. HaCaT cells were then treated with TNF-α with 16D10 or TPCA-1 for 20 min. The cells were fixed by 4% paraformaldehyde (PFA) for 15 min and permeabilized with 0.5% Triton X-100 for 10 min. After permeabilization, the cells were incubated with 1% BSA-PBS blocking solution for 60 min, and then incubated overnight at 4°C with anti-p65 antibody. After incubation with anti-p65 antibody, the cells were incubated with DAPI, and then incubated in the dark with secondary antibody, Alexa Fluor 488 (A-11070) for 1 h at room temperature. Cell images were obtained using an LSM700 instrument (Zeiss, Go¨ttingen, Germany). The number of total cells and p65 nuclear translocated cells were counted from four high-power fields (×150) in each group. The percentage of the p65 nuclei-positive cells to the total cells was determined.

*2.11 siRNA treatment*

HaCaT cells were seeded in KGM medium at a density of $0.25\text{-}5 \times 10^5$ cells/well in 24-well plates. Nrf2 MISSION esiRNA was transfected 2 days after seeding and Keap1 MISSION esiRNA was transfected 1 day after seeding using the Lipofectamine RNAiMAX Transfection Reagent. The cells were incubated for 24 h after Nrf2 MISSION esiRNA transfection or 72 h after Keap1 MISSION esiRNA transfection. Then, HaCaT cells were treated with TNF-α and 16D10 (10 μM) for 2 h.

*2.12 LPS-induced air-pouch-type inflammation*

Male BALB/c mice (5-7 weeks old) were subcutaneously injected with 0.5 ml of air on the dorsum to form an oval-shaped air pouch. To maintain the shape of the air pouches, 0.5 ml of air was injected into the air pouches 3-4 times a week. Eight days after the first air injection, 0.3 ml sterile solution with 2 % (w/v) sodium carboxymethyl cellulose (CMC-Na, Daiichi Kogyo, Niigata, Japan) in saline containing 10 ng/ml LPS or 0.5 ml sterile solution with 2% (w/v) CMC-Na in saline containing 200 μg/ml OVA with 16D10 (0.3 and 1 mM) and antibiotics (0.1 mg/ml penicillin G potassium and 0.1 mg/ml streptomycin sulfate) were injected into the air pouch of each mouse. After 8 h, the mice were killed by severing the carotid artery under anesthesia by isoflurane inhalation. The pouch fluid from each mouse was collected. The collected pouch fluids were diluted two-fold with ice-cold saline and centrifuged at 1500 ×*g* and 4 °C for 10 min. The supernatant was used to determine the levels of TSLP in the pouch fluids.

*2.13 OVA-induced air-pouch-type inflammation and sensitization model*

Male ICR mice (5-7 weeks old) were subcutaneously injected with 0.5 ml air on the dorsum to form oval-shaped air pouch (day 0). To maintain the shape of air pouches, 0.5 ml air was injected every second day (day 2, 4, 6). On day 7, 0.5 ml sterile solution with 2% CMC-Na in saline containing 200 μg/ml OVA with 16D10 (1 mM) and antibiotics mentioned above were injected into the air pouch in each mouse. In this OVA-induced air-pouch-type inflammation model, the mice were killed 8 h after the injection and the pouch fluids were collected as described above. In the OVA-induced air-pouch-type sensitization model, 0.2 ml 16D10 (1 mM) in saline was injected every second day from day 8 to day 20. To evaluate the induction of OVA-specific

antibodies, mice were killed 14 days after OVA injection and serum samples were collected.

*2.14 Statistical analysis*

All data are expressed as means ± standard error of the means (S.E.M.). A two-tailed paired Student's t test was performed to compare data between the two groups. Dunnett's test was carried out for multiple comparisons.

## 3. Results

*3.1 16D10 inhibited TSLP production in KCMH-1 cells*

From the 2169 chemical compounds screened in KCMH-1 cells, constitutively producing TSLP, we identified a chalcone derivative, with code no. 16D10. The structure of 16D10 is shown in Fig. 1A. Treatment with 16D10 for 24 h did not affect the viability of KCMH-1 cells (Fig. 1B) but significantly inhibited TSLP production in KCMH-1 cells in a concentration-dependent manner (Fig. 1C). Treatment with 16D10 (10 μM) also suppressed TSLP mRNA expression in KCMH-1 cells (Fig. 1D).

*3.2 Chalcone structure is important for the inhibition of TSLP production*

To determine the key structure for the inhibition of TSLP production, we used three chemical compounds which have the part structure of 16D10 (Fig. 2A). We examined the effects of these chemical compounds on TSLP production in KCMH-1 cells, and found that only STK381202, which has a chalcone structure, significantly inhibited TSLP production although its activity was weaker than that of 16D10 (Fig. 2B).

*3.3 16D10 inhibited TSLP expression in a human keratinocyte cell line*

To confirm whether 16D10 suppresses TSLP expression in human keratinocytes, we investigated the effect of 16D10 on TSLP expression in HaCaT cells, a human keratinocyte cell line. Since poly(I:C) and TNF-α are known to induce TSLP expression in human epithelial cells (Xie et al., 2012), we used these as TSLP inducers. 16D10 significantly inhibited TSLP expression induced by both poly(I:C) and TNF-α (Fig. 3A and 3B). To confirm the effects of 16D10 on TSLP promoter activation, we prepared two TSLP promoter reporter plasmids, one with promoter region -4102 to +185 and the other with region -259 to +185. TNF-α induced the activation of both promoter regions, and 16D10 significantly inhibited both (Fig. 3C).

*3.4 16D10 did not directly inhibit NF-κB activation*

NF-κB is a key transcription factor for TSLP induction (Cultrone et al., 2013; Redhu et al., 2011). Therefore, we examined the effects of 16D10 on NF-κB activation, which was assessed by IκB degradation, translocation of NF-κB p65 into nucleus, and NF-κB reporter gene assay. TPCA-1, a selective inhibitor of IκB kinase, potently inhibited TNF-α-induced IκBα degradation (Fig. 4A), and translocation of p65 in HaCaT cells (Fig. 4B and 4C). 16D10 did not inhibit these even at 100 μM (Fig. 4A-C). Furthermore, the increase in NF-κB dependent transcription induced by TNF-α was not inhibited by 16D10 to an extent high enough to potently inhibit TSLP production in HaCaT cells (Fig. 4C). This was also true in mouse KCMH-1 cells, in which 16D10 did not inhibit NF-κB reporter activity, although TPCA-1 significantly suppressed it (Fig. 4D).

*3.5 16D10 activated the Keap1-Nrf2 system although this pathway was not involved in the inhibition of TSLP production in HaCaT cells*

Certain chalcone structure compounds activates Nrf2 signaling and protect against oxidative stress (Kumar et al., 2011; Yao et al., 2015). In addition, Nrf2 suppresses the transcription of certain proinflammatory cytokines in mouse macrophages (Kobayashi et al., 2016). Therefore, we analyzed the involvement of the Keap1-Nrf2 system in the suppression of TSLP expression by 16D10 in HaCaT cells. 16D10 increased Nrf2 expression from 1 to 4 h after the treatment, similarly to DEM, a known Nrf2 activator (Fig. 5A). To clarify whether the activated Nrf2 pathway was involved in the inhibitory activity of 16D10 on TSLP expression, we examined the effects of Nrf2 and Keap1 knockdown via esiRNA on TSLP expression. Hemeoxygenase-1 (HMOX1), a marker of Nrf2 activation, was upregulated by 16D10, and its expression was completely downregulated by Nrf2 esiRNA (Fig. 5B). Treatment of HaCaT cells with Nrf2 esiRNA significantly upregulated TNF-α-induced TSLP mRNA expression but did not prevent the inhibitory action of 16D10 (Fig. 5C). Nrf2 activation was also induced by the reduction of Keap1 via Keap1 esiRNA. Furthermore, Keap1 esiRNA induced HMOX1 mRNA expression in both presence and absence of TNF-α. Keap1 esiRNA, however, did not affect TNF-α-induced TSLP mRNA expression (Fig. 5D and 5E), indicating that the activation of Nrf2 did not cause the reduction of TSLP expression.

*3.6 16D10 inhibited the production of TSLP induced by LPS or OVA in vivo*

To clarify the effect of 16D10 on TSLP production *in vivo*, we used an air-pouch-type inflammation model, in which TSLP production can be assessed quantitatively (Segawa et al., 2016). A diagrammatic representation of the LPS-induced air-pouch-type

inflammation model is shown in Fig. 6A. TSLP levels in pouch fluids collected at 8 h after LPS stimulation were determined. 16D10 (0.3 and 1 mM) significantly reduced TSLP levels in pouch fluid in a concentration-dependent manner (Fig. 6B). Furthermore, we confirmed the inhibitory effects of 16D10 on TSLP production induced by the injection of OVA into the air pouch. A diagrammatic representation of the OVA-induced air-pouch-type inflammation model is shown in Fig. 6C. In Fig. 6D, the levels of TSLP in pouch fluids were significantly decreased by 16D10 treatment as well as were those in the LPS-induced model. However, the levels of TNF-α and IL-1β, which are intrinsic inducers of TSLP production, were not affected by 16D10 treatment (Fig. 6D, middle and right graph).

### *3.7 16D10 inhibited TSLP and antibody production in an OVA-induced air-pouch-type allergy model*

To evaluate the effect of 16D10 on immunological sensitization, we set up an air-pouch-type OVA sensitization model. A diagrammatic representation of this model is shown in Fig. 7A. In this model, the injection of OVA (100 μg) into the air pouch increased OVA-specific IgG1 and IgE levels after 21 days. As shown in Fig. 7B, the repeated injection of 16D10 (1 mM) into the pouch on day 7 (with immunization) and every second day from day 8 to day 20 significantly reduced the levels of OVA-specific IgG1 and IgE measured in the serum on day 21. The inhibitory action of 16D10 on IgE production was also observed in the case of the single application at the immunization with OVA (Fig. 7C and 7D).

## 4. Discussion

In this study, we identified 16D10 as an inhibitor of TSLP production from a compound library screen conducted in KCMH-1 cells. 16D10 inhibited TSLP expression in the mouse and human keratinocyte cell lines, KCMH-1 and HaCaT. 16D10 inhibited TSLP production selectively via unidentified mechanisms other than direct inhibition of NF-κB and activation of the Keap1-Nrf2 system. Importantly, 16D10 inhibited TSLP and OVA-specific IgG1 and IgE expression *in vivo*. Thus, 16D10 could be a lead compound for novel anti-allergic medicines.

NF-κB is the main regulator of TSLP expression. For example, TNF-α induced the expression of TSLP through NF-κB activation (Redhu et al., 2011). Peroxisome proliferator-activated receptor β/δ agonists and aryl hydrocarbon receptor agonists inhibited TSLP production by the inhibition of NF-κB p65 acetylation in human keratinocyte cell lines (Barroso et al., 2011; Jeong et al., 2018). RXR directly binding NF-κB and suppressed TSLP expression in a human bronchial epithelial cell line (Lee et al., 2008). In addition, several chalcone derivatives have the ability to inhibit cytokine production by inhibiting the NF-κB activation pathway (Chen et al., 2018; Li et al., 2015). However, 16D10 did not inhibit TNF-α-induced IκB degradation, translocation of NF-κB p65 into the nucleus, or NF-κB promoter activation at the concentration at which it showed strong inhibitory effects on TSLP production in HaCaT cells, indicating that 16D10 did not inhibit the NF-κB activation pathway. These results were supported by the findings that 16D10 did not inhibit TNF-α and IL-1β production *in vivo*.

AP-1 also involves the transcriptional induction of TSLP by Notch ligands and TNF-α (Murthy et al., 2012; Redhu et al., 2011). 16D10, however, did not affect phosphorylation of MAPKs (ERK, p38, JNK) and AP-1 reporter activation was not

induced by TNF-α in HaCaT cells (data not shown). Therefore, 16D10 will not be affected AP-1 activation.

Glucocorticoid negatively regulates TSLP expression via negative glucocorticoid response element (nGRE) (Hudson et al., 2013). In contrast, HIF-1α (hypoxia inducible factor-1α) positively regulates TSLP expression via HRE (hypoxia response element) in human TSLP promoter region (Jang et al., 2013). The reporter gene assay performed here using the promoter region of -259 to +185, in which the nGRE and HRE were not included, indicated that the effects of 16D10 affected unknown signaling except for GR/nGRE and HIF-1α/HRE activation.

We found that 16D10 induced Nrf2 activation. Nrf2 is a transcription factor that mainly regulates anti-oxidant factor expression (Ferrándiz et al., 2018). Nrf2 expression is constitutively down-regulated by Keap1, which binds to Nrf2 and promotes degradation of it. When Keap1 recognizes electrophiles and reactive oxygen species with cysteine residues, Nrf2 is released from Keap1 and activated. Several chalcone derivatives activate Keap1-Nrf2 system and promote redox reactions (Kumar et al., 2011; Yao et al., 2015). Recently, Kobayashi EH et al. suggested that Nrf2 inhibited the expression of pro-inflammatory cytokines in mouse macrophages and that this inhibition was independent of the Nrf2-binding motif and reactive oxygen species levels (Kobayashi et al., 2016). However, we concluded that 16D10-induced Nrf2 activation was not involved in the inhibition of TSLP expression in HaCaT cells from the following findings. First, Nrf2 knockdown inhibited Nrf2-dependent expression of HMOX1 but did not affect the inhibitory effect of 16D10. Second, the activation of Nrf2 via down-regulation of Keap1 enhanced the Nrf2-dependent expression of HMOX1 but did not affected the expression of TSLP. The possibility that the baseline

level of Nrf2 negatively regulated TSLP expression was not denied because Nrf2 knockdown significantly up-regulated TNF-α-induced, but not baseline, TSLP expression.

Taken together, these results indicate that 16D10 may have a novel target to regulate TSLP expression. The identification of the target and optimization of 16D10 are in progress in our laboratory.

We confirmed that 16D10 inhibited TSLP production *in vivo*. We already reported that TSLP production in LPS-induced air-pouch-type inflammation was produced in air-pouch-formed skin (Segawa et al., 2016). The administration of 16D10 into the air pouch inhibited LPS- and OVA-induced TSLP production significantly, indicating that 16D10 inhibited TSLP production in keratinocytes in these models. Importantly, 16D10 did not reduce the levels of TNF-α and IL-1β, which are intrinsic TSLP inducers and induced by NF-κB activation (Lee et al., 2008; Redhu et al., 2011), in the OVA-induced air-pouch-type inflammation model. This indicates that 16D10 did not inhibit NF-κB activation, which induces the production of TNF-α and IL-1β *in vivo*. TSLP enhances production of Th2-type cytokines and antibodies production in several allergy models in mice (He et al., 2008; Shen et al., 2017; Zhou et al., 2005). TSLP also affects immunoglobulin class switching (Xu et al., 2007). Corresponding with these reports, we demonstrated that repetitive administration of 16D10 inhibited the induction of OVA-specific IgG1 and IgE, which are markers for Th2 responses, in the air-pouch-type sensitization model in mice. Further, single administration of 16D10 at the time of OVA-sensitization also inhibited the induction of OVA-specific IgE. These results suggest that the suppression of TSLP production in the time of OVA-sensitization by 16D10 leads to the suppression of antibodies production. Hence,

16D10 would exert anti-allergic effects by inhibiting TSLP production.

This is the first study showing that the selective inhibitor of TSLP reduces antigen-specific antibodies production. TSLP is a key epithelial-derived cytokine that aggravates allergic diseases. Recently, it was reported that tezepelumab, an antibody specific for TSLP, is effective in the prevention of asthma exacerbation in patients with moderate to severe asthma (Corren et al., 2017). Recently, a phase Ⅱa clinical trial in patients with moderate to severe atopic dermatitis. The regulation of TSLP production is therefore an expected strategy for the treatment of allergic diseases, and selective inhibitors of TSLP production will support conventional therapy. Steroids and tacrolimus, an immunosuppressive agent, are first-choice medicines for the treatment of allergic diseases. Steroids, but not tacrolimus, suppress TSLP production in an atopic dermatitis model of mice and in primary human keratinocytes (Mizuno et al., 2015). However, steroid and tacrolimus strongly inhibited immune responses, resulting in an increased susceptibility to infection. TSLP is not involved in the induction of inflammation and natural immunity. Furthermore, as epithelial cells are a major source of TSLP, TSLP inhibitor can exert potent effects via local application. Thus, an inhibitor of TSLP production would be a medicine with fewer side effects than steroids and tacrolimus. Another problem with steroid treatment is unresponsiveness to steroids, called steroid resistance. TSLP induces steroid resistance in type 2 innate lymphoid cells (ILC2) via the signal transducers and activators of transcription (STAT) and MEK signaling pathway in allergic asthma (Kabata et al., 2013; Liu et al., 2018). Therefore, an inhibitor of TSLP production could help to restore responsiveness to steroids. Taken together, these results suggest that TSLP production inhibitors will be the next-generation of anti-allergic drugs.

## 5. Conclusions

16D10 inhibits TSLP production by unreported mechanisms and has potential as a medicine for allergic diseases. Further studies based on this finding is useful to understand more detail regulation of TSLP expression and to find new treatment targets for allergic diseases.


## Acknowledgements

This work was funded in part Grant-in-aid of Challenging Exploratory Research (17K19470) from the Japan Society for the Promotion of Science and the Translational Research Network Program from the Japan Agency for Medical Research and Development.


## Conflict of Interest

The authors declare no conflicts of interest.

## 6. References


Allakhverdi, Z., Comeau, M.R., Jessup, H.K., Yoon, B.-R.P., Brewer, A., Chartier, S., Paquette, N., Ziegler, S.F., Sarfati, M., Delespesse, G., 2007. Thymic stromal lymphopoietin is released by human epithelial cells in response to microbes, trauma, or inflammation and potently activates mast cells. J. Exp. Med. 204, 253–8. https://doi.org/10.1084/jem.20062211

Ashcroft, D.M., 2005. Efficacy and tolerability of topical pimecrolimus and tacrolimus in the treatment of atopic dermatitis: meta-analysis of randomised controlled trials. Bmj 330, 516–0. https://doi.org/10.1136/bmj.38376.439653.D3

Barroso, E., Eyre, E., Palomer, X., Vázquez-Carrera, M., 2011. The peroxisome proliferator-activated receptor β/δ (PPARβ/δ) agonist GW501516 prevents TNF-α-induced NF-κB activation in human HaCaT cells by reducing p65 acetylation through AMPK and SIRT1. Biochem. Pharmacol. 81, 534–543. https://doi.org/10.1016/j.bcp.2010.12.004

Boguniewicz, M., Alexis, A.F., Beck, L.A., Block, J., Eichenfield, L.F., Fonacier, L., Guttman-Yassky, E., Paller, A.S., Pariser, D., Silverberg, J.I., Lebwohl, M., 2017. Expert Perspectives on Management of Moderate-to-Severe Atopic Dermatitis: A Multidisciplinary Consensus Addressing Current and Emerging Therapies. J. Allergy Clin. Immunol. Pract. 5, 1519–1531. https://doi.org/10.1016/j.jaip.2017.08.005

Chen, X., Yu, W., Li, W., Zhang, H., Huang, W., Wang, J., Zhu, W., Fang, Q., Chen, C., Li, X., Liang, G., 2018. An anti-inflammatory chalcone derivative prevents heart and kidney from hyperlipidemia-induced injuries by attenuating inflammation. Toxicol. Appl. Pharmacol. 338, 43–53. https://doi.org/10.1016/j.taap.2017.11.003

Corren, J., Parnes, J.R., Wang, L., Mo, M., Roseti, S.L., Griffiths, J.M., van der Merwe, R., 2017. Tezepelumab in Adults with Uncontrolled Asthma. N. Engl. J. Med. 377, 936–946. https://doi.org/10.1056/NEJMoa1704064

Cultrone, A., de Wouters, T., Lakhdari, O., Kelly, D., Mulder, I., Logan, E., Lapaque, N., Doré, J., Blottière, H.M., 2013. The NF-κB binding site located in the proximal region of the TSLP promoter is critical for TSLP modulation in human intestinal epithelial cells. Eur. J. Immunol. 43, 1053–1062. https://doi.org/10.1002/eji.201142340

Eckert, L., Gupta, S., Amand, C., Gadkari, A., Mahajan, P., Gelfand, J.M., 2018. The burden of atopic dermatitis in US adults: Health care resource utilization data from the 2013 National Health and Wellness Survey. J. Am. Acad. Dermatol. 78, 54–61.e1. https://doi.org/10.1016/j.jaad.2017.08.002

Ferrándiz, M.L., Nacher-Juan, J., Alcaraz, M.J., 2018. Nrf2 as a therapeutic target for rheumatic diseases. Biochem. Pharmacol. 152, 338–346. https://doi.org/10.1016/j.bcp.2018.04.010

Gauvreau, G.M., O'Byrne, P.M., Boulet, L.-P., Wang, Y., Cockcroft, D., Bigler, J., FitzGerald, J.M., Boedigheimer, M., Davis, B.E., Dias, C., Gorski, K.S., Smith, L., Bautista, E., Comeau, M.R., Leigh, R., Parnes, J.R., 2014. Effects of an anti-TSLP antibody on allergen-induced asthmatic responses. N. Engl. J. Med. 370, 2102–10. https://doi.org/10.1056/NEJMoa1402895

Harada, M., Hirota, T., Jodo, A.I., Doi, S., Kameda, M., Fujita, K., Miyatake, A., Enomoto, T., Noguchi, E., Yoshihara, S., Ebisawa, M., Saito, H., Matsumoto, K., Nakamura, Y., Ziegler, S.F., Tamari, M., 2009. Functional analysis of the thymic stromal lymphopoietin variants in human bronchial epithelial cells. Am. J. Respir.

Cell Mol. Biol. 40, 368–374. https://doi.org/10.1165/rcmb.2008-0041OC

He, R., Oyoshi, M.K., Garibyan, L., Kumar, L., Ziegler, S.F., Geha, R.S., 2008. TSLP acts on infiltrating effector T cells to drive allergic skin inflammation. Proc. Natl. Acad. Sci. U. S. A. 105, 11875–80. https://doi.org/10.1073/pnas.0801532105

Hoare, C., Li Wan Po, A., Williams, H., 2000. Systematic review of treatments for atopic eczema. Health Technol. Assess. (Rockv). 4. https://doi.org/10.1016/S0190-9622(02)61464-1

Hudson, W.H., Youn, C., Ortlund, E.A., 2013. The structural basis of direct glucocorticoid-mediated transrepression. Nat. Struct. Mol. Biol. 20, 53–58. https://doi.org/10.1038/nsmb.2456

Jang, Y., Jeong, S.H., Park, Y.H., Bae, H.C., Lee, H., Ryu, W.I., Park, G.H., Son, S.W., 2013. UVB induces HIF-1α-dependent TSLP expression via the JNK and ERK pathways. J. Invest. Dermatol. 133, 2601–2608. https://doi.org/10.1038/jid.2013.203

Jeong, H., Shin, J.Y., Kim, M.-J., Na, J., Ju, B.-G., 2018. Activation of aryl hydrocarbon receptor negatively regulates thymic stromal lymphopoietin gene expression via PKCδ-p300- NF-κB pathway in keratinocytes under inflammatory conditions. J. Invest. Dermatol. https://doi.org/10.1016/j.jid.2018.11.012

Jiang, H., Hener, P., Li, J., Li, M., 2012. Skin thymic stromal lymphopoietin promotes airway sensitization to inhalant house dust mites leading to allergic asthma in mice. Allergy 67, 1078–82. https://doi.org/10.1111/j.1398-9995.2012.02857.x

Jiang, X.-Y., Zhao, J.-H., Yu, C.-X., Fang, L., Zheng, X.-D., Yin, X.-Y., Wu, Y.-Y., Tang, X.-F., Zhou, F.-S., Zhang, X.-J., Xiao, F.-L., 2017. Association analyses identify two susceptibility loci 5q31 and 5q22.1 for atopic dermatitis in Chinese

Han population. Asian Pacific J. allergy Immunol. https://doi.org/10.12932/AP0869

Kabata, H., Moro, K., Fukunaga, K., Suzuki, Y., Miyata, J., Masaki, K., Betsuyaku, T., Koyasu, S., Asano, K., 2013. Thymic stromal lymphopoietin induces corticosteroid resistance in natural helper cells during airway inflammation. Nat. Commun. 4, 2675. https://doi.org/10.1038/ncomms3675

Kobayashi, E.H., Suzuki, T., Funayama, R., Nagashima, T., Hayashi, M., Sekine, H., Tanaka, N., Moriguchi, T., Motohashi, H., Nakayama, K., Yamamoto, M., 2016. Nrf2 suppresses macrophage inflammatory response by blocking proinflammatory cytokine transcription. Nat. Commun. 7, 1–14. https://doi.org/10.1038/ncomms11624

Kumar, V., Kumar, S., Hassan, M., Wu, H., Thimmulappa, R.K., Kumar, A., Sharma, S.K., Parmar, V.S., Biswal, S., Malhotra, S. V., 2011. Novel chalcone derivatives as potent Nrf2 activators in mice and human lung epithelial cells. J. Med. Chem. 54, 4147–4159. https://doi.org/10.1021/jm2002348

Lee, H.-C., Headley, M.B., Iseki, M., Ikuta, K., Ziegler, S.F., 2008. Cutting edge: Inhibition of NF-kappaB-mediated TSLP expression by retinoid X receptor. J. Immunol. 181, 5189–93. https://doi.org/10.4049/jimmunol.181.8.5189

Li, Y.Y., Huang, S.S., Lee, M.M., Deng, J.S., Huang, G.J., 2015. Anti-inflammatory activities of cardamonin from Alpinia katsumadai through heme oxygenase-1 induction and inhibition of NF-κB and MAPK signaling pathway in the carrageenan-induced paw edema. Int. Immunopharmacol. 25, 332–339. https://doi.org/10.1016/j.intimp.2015.02.002

Liu, S., Verma, M., Michalec, L., Liu, W., Sripada, A., Rollins, D., Good, J., Ito, Y.,

Chu, H.W., Gorska, M.M., Martin, R.J., Alam, R., 2018. Steroid resistance of airway type 2 innate lymphoid cells from patients with severe asthma: The role of thymic stromal lymphopoietin. J. Allergy Clin. Immunol. 141, 257–268.e6. https://doi.org/10.1016/j.jaci.2017.03.032

Lowe, A.J., Leung, D.Y.M., Tang, M.L.K., Su, J.C., Allen, K.J., 2018. The skin as a target for prevention of the atopic march. Ann. Allergy, Asthma Immunol. 120, 145–151. https://doi.org/10.1016/j.anai.2017.11.023

Mizuno, K., Morizane, S., Takiguchi, T., Iwatsuki, K., 2015. Dexamethasone but not tacrolimus suppresses TNF-α-induced thymic stromal lymphopoietin expression in lesional keratinocytes of atopic dermatitis model. J. Dermatol. Sci. 80, 45–53. https://doi.org/10.1016/j.jdermsci.2015.06.016

Murthy, A., Shao, Y.W., Narala, S.R., Molyneux, S.D., Zúñiga-Pflücker, J.C., Khokha, R., 2012. Notch activation by the metalloproteinase ADAM17 regulates myeloproliferation and atopic barrier immunity by suppressing epithelial cytokine synthesis. Immunity 36, 105–19. https://doi.org/10.1016/j.immuni.2012.01.005

Omori-Miyake, M., Ziegler, S.F., 2012. Mouse Models of Allergic Diseases: TSLP and Its Functional Roles. Allergol. Int. 61, 27–34. https://doi.org/10.2332/allergolint.11-RAI-0374

Redhu, N.S., Saleh, A., Halayko, A.J., Ali, A.S., Gounni, A.S., 2011. Essential role of NF-κB and AP-1 transcription factors in TNF-α-induced TSLP expression in human airway smooth muscle cells. Am. J. Physiol. Lung Cell. Mol. Physiol. 300, L479-85. https://doi.org/10.1152/ajplung.00301.2009

Salter, B.M., Oliveria, J.P., Nusca, G., Smith, S.G., Watson, R.M., Comeau, M., Sehmi, R., Gauvreau, G.M., 2015. Thymic stromal lymphopoietin activation of basophils

in patients with allergic asthma is IL-3 dependent. J. Allergy Clin. Immunol. 136, 1636–1644. https://doi.org/10.1016/j.jaci.2015.03.039

Segawa, R., Mizuno, N., Hatayama, T., Jiangxu, D., Hiratsuka, M., Endo, Y., Hirasawa, N., 2016. Lipopolysaccharide-Activated Leukocytes Enhance Thymic Stromal Lymphopoietin Production in a Mouse Air-Pouch-Type Inflammation Model. Inflammation 39, 1527–1537. https://doi.org/10.1007/s10753-016-0388-1

Segawa, R., Yamashita, S., Mizuno, N., Shiraki, M., Hatayama, T., Satou, N., Hiratsuka, M., Hide, M., Hirasawa, N., 2014. Identification of a cell line producing high levels of TSLP: advantages for screening of anti-allergic drugs. J. Immunol. Methods 402, 9–14. https://doi.org/10.1016/j.jim.2013.10.012

Shen, S., Li, J., You, H., Wu, Z., Wu, Y., Zhao, Y., Zhu, Y., Guo, Q., Li, X., Li, R., Ma, P., Yang, X., Chen, M., 2017. Oral exposure to diisodecyl phthalate aggravates allergic dermatitis by oxidative stress and enhancement of thymic stromal lymphopoietin. Food Chem. Toxicol. 99, 60–69. https://doi.org/10.1016/j.fct.2016.11.016

Siegfried, E.C., Jaworski, J.C., Kaiser, J.D., Hebert, A.A., 2016. Systematic review of published trials: Long-term safety of topical corticosteroids and topical calcineurin inhibitors in pediatric patients with atopic dermatitis. BMC Pediatr. 16, 1–15. https://doi.org/10.1186/s12887-016-0607-9

Soumelis, V., Reche, P. a, Kanzler, H., Yuan, W., Edward, G., Homey, B., Gilliet, M., Ho, S., Antonenko, S., Lauerma, A., Smith, K., Gorman, D., Zurawski, S., Abrams, J., Menon, S., McClanahan, T., de Waal-Malefyt Rd, R., Bazan, F., Kastelein, R. a, Liu, Y.-J., 2002. Human epithelial cells trigger dendritic cell mediated allergic inflammation by producing TSLP. Nat. Immunol. 3, 673–80.

https://doi.org/10.1038/ni805

Tatsuno, K., Fujiyama, T., Yamaguchi, H., Waki, M., Tokura, Y., 2015. TSLP Directly Interacts with Skin-Homing Th2 Cells Highly Expressing its Receptor to Enhance IL-4 Production in Atopic Dermatitis. J. Invest. Dermatol. 1–33. https://doi.org/10.1038/jid.2015.318

Torgerson, D.G., Ampleford, E.J., Chiu, G.Y., Gauderman, W.J., Gignoux, C.R., Graves, P.E., Himes, B.E., Levin, A.M., Mathias, R.A., Hancock, D.B., Baurley, J.W., Eng, C., Stern, D.A., Celedón, J.C., Rafaels, N., Capurso, D., Conti, D. V, Roth, L.A., Soto-Quiros, M., Togias, A., Li, X.X., Myers, R.A., Romieu, I., Van Den Berg, D.J., Hu, D., Hansel, N.N., Hernandez, R.D., Israel, E., Salam, M.T., Galanter, J., Avila, P.C., Avila, L., Rodriquez-Santana, J.R., Chapela, R., Rodriguez-Cintron, W., Diette, G.B., Adkinson, N.F., Abel, R.A., Ross, K.D., Shi, M., Faruque, M.U., Dunston, G.M., Watson, H.R., Mantese, V.J., Ezurum, S.C., Liang, L., Ruczinski, I., Ford, J.G., Huntsman, S., Chung, K.F., Vora, H., Li, X.X., Calhoun, W.J., Castro, M., Sienra-Monge, J.J., del Rio-Navarro, B., Deichmann, K.A., Heinzmann, A., Wenzel, S.E., Busse, W.W., Gern, J.E., Lemanske, R.F., Beaty, T.H., Bleecker, E.R., Raby, B.A., Meyers, D.A., London, S.J., Gilliland, F.D., Burchard, E.G., Martinez, F.D., Weiss, S.T., Williams, L.K., Barnes, K.C., Ober, C., Nicolae, D.L., 2011. Meta-analysis of genome-wide association studies of asthma in ethnically diverse North American populations. Nat Genet 43, 887–892. https://doi.org/10.1038/ng.888

Weidinger, S., Novak, N., 2016. Atopic dermatitis. Lancet 387, 1109–1122. https://doi.org/10.1016/S0140-6736(15)00149-X

Xie, Y., Takai, T., Chen, X., Okumura, K., Ogawa, H., 2012. Long TSLP transcript

expression and release of TSLP induced by TLR ligands and cytokines in human keratinocytes. J. Dermatol. Sci. 66, 233–237. https://doi.org/10.1016/j.jdermsci.2012.03.007

Xu, W., He, B., Chiu, A., Chadburn, A., Shan, M., Buldys, M., Ding, A., Knowles, D.M., Santini, P.A., Cerutti, A., 2007. Epithelial cells trigger frontline immunoglobulin class switching through a pathway regulated by the inhibitor SLPI. Nat. Immunol. 8, 294–303. https://doi.org/10.1038/ni1434

Yao, J., Zhang, B., Ge, C., Peng, S., Fang, J., 2015. Xanthohumol, a polyphenol chalcone present in hops, activating nrf2 enzymes to confer protection against oxidative damage in pc12 cells. J. Agric. Food Chem. 63, 1521–1531. https://doi.org/10.1021/jf505075n

Zhou, B., Comeau, M.R., De Smedt, T., Liggitt, H.D., Dahl, M.E., Lewis, D.B., Gyarmati, D., Aye, T., Campbell, D.J., Ziegler, S.F., 2005. Thymic stromal lymphopoietin as a key initiator of allergic airway inflammation in mice. Nat. Immunol. 6, 1047–53. https://doi.org/10.1038/ni1247

Ziegler, S.F., Artis, D., 2010. Sensing the outside world: TSLP regulates barrier immunity. Nat. Immunol. 11, 289–293. https://doi.org/10.1038/ni.1852

## Figure legends

**Fig. 1. 16D10 inhibits TSLP production in KCMH-1 cells.**

(A) The chemical structure of 16D10. (B-D) KCMH-1 cells were treated with 16D10 at the indicated concentrations for 24 h (B and C) or 8 h (D). The viability of KCMH-1 cells (B), the concentration of TSLP in the culture media (C), and the expression of TSLP mRNA (D) were determined. All data are represented as means ± S.E.M. (n=4). $^{**}P < 0.01$ vs. DMSO group (control). n.s.: not significant

**Fig.2. Chalcone structure is important for the inhibition of TSLP production.**

(A) The structure of compounds that have substructures related to that of 16D10. (B) KCMH-1 cells were treated with each compound (1, 3, and 10 μM) and the concentration of TSLP in the culture media at 24 h was quantified by ELISA. All data are represented as means ± S.E.M. (n=4). $^{**}P < 0.01$ vs. DMSO group (control). n.s.: not significant

**Fig. 3. 16D10 inhibits expression of TSLP mRNA and TSLP promoter activation in HaCaT cells.**

(A and B) HaCaT cells were stimulated with 50 μg/ml poly(I:C) (A) or 100 ng/ml TNF-α (B) in the presence of 10 μM 16D10. The expression of TSLP mRNA in HaCaT cells 4 h were determined by qPCR. (C and D) HaCaT cells were transiently transfected with reporter constructs, which include -4102 to +185 of TSLP promoter (C) or -259 to +185 (D), and 24 h later, stimulated with TNF-α (100 ng/ml) with 16D10 (10 μM) for 2 h. *Firefly* luciferase activity was normalized to *Renilla* luciferase activity

and normalized values were calculated as fold-change compared to the control group. All data are represented as means ± S.E.M. (n=3-4). $^{**}P < 0.01$ vs. control group, $^{\#}P < 0.05$, $^{\#\#}P < 0.01$ vs. TNF-α alone group.

**Fig. 4. 16D10 did not inhibit NF-κB activation.**

(A and B) HaCaT cells were stimulated with TNF- $\alpha$ (100 ng/ml) in the presence of 16D10 (10, 30, and 100 μM) or TPCA-1 (10 μM) for 20 min. The expression of IκB (A) and (B) translocation of p65 were determined. (C) The percentage of nuclear p65 positive cells per total cells. (D) HaCaT cells were transiently transfected with NF-κB luciferase reporter constructs, and 24 h later, stimulated for 2 h with TNF-α (100 ng/ml) in the presence of 16D10 (10 μM). *Firefly* luciferase activity was normalized to *Renilla* luciferase activity. (E) KCMH-1 cells were transiently transfected with NF-κB luciferase reporter constructs, and 12 h later, treated with 16D10 (1, 3, and 10 μM) or TPCA-1 (3 μM) for 12 h. *Firefly* luciferase activity was normalized to *Renilla* luciferase activity. Data are represented as means± S.E.M. (n=3-4). $^{*}P < 0.05$ vs. control group. $^{\#\#}P < 0.01$ vs. TNF-α alone group. TP: TPCA-1 (10 μM). n.s.: not significant

**Fig. 5. 16D10 activates Nrf2 signaling, although Nrf2 is involved in the inhibition of TSLP production**

(A) HaCaT cells were stimulated with 16D10 (10 μM) or DEM (100 μM) for 1, 2, and 4 h. The expression of Nrf2 protein in HaCaT cells was analyzed by western blot. (B and C) Nrf2 or control siRNA was transfected 24 h before treatment with TNF-α (100 ng/ml) and 16D10 (10 μM). The expression of HMOX-1 (B) and TSLP (C) mRNA in

HaCaT cells 2 h after the treatment was determined by qPCR. (D and E) Keap1 or control siRNA was transfected 72 h before treatment with TNF-α (100 ng/ml). The expression of HMOX-1 (D) and TSLP (E) mRNA in HaCaT cells 2 h after stimulation with TNF-α (100 ng/ml) was determined by qPCR. Data are represented as means± S.E.M. (n=3-4). $^{*}P < 0.05$, $^{**}P < 0.01$ vs. corresponding group transfected with control siRNA, $^{\#\#}P < 0.01$ vs. Nrf2 siRNA transfected TNF-α alone group. n.s.: not significant

**Fig. 6. 16D10 inhibits TSLP production in an LPS- or OVA-induced air-pouch-type inflammation model.**

(A) Diagrammatic representation of the LPS-induced air-pouch-type inflammation model. (B) LPS (10 ng/ml) and 16D10 (0.3 or 1 mM), in 0.5 ml sterile solution with 2% (w/v) CMC-Na was injected into the pre-formed air-pouches in mice. The levels of TSLP in the pouch fluid samples collected 8 h after the injection of LPS were quantified by ELISA. (C) Diagrammatic representation of the OVA-induced air-pouch-type inflammation model. (D) OVA (200 μg/ml) and 16D10 (1 mM), in 0.5 ml sterile solution with 2% (w/v) CMC-Na was injected into the pre-formed air-pouches of mice. The levels of TSLP, IL-1β, and TNF-α in the pouch fluid samples collected 8 h after the injection of OVA were quantified by ELISA. Data are represented as means ± S.E.M. (n=6-7). $^{**}P < 0.01$ vs. control group, $^{\#}P < 0.05$, $^{\#\#}P < 0.01$ vs. LPS or OVA alone group. n.s.: not significant

**Fig. 7. 16D10 inhibits antibodies production in OVA-induced air-pouch-type allergy model.**

(A) Diagrammatic representation of the OVA-induced air-pouch-type allergy model. (B) OVA (200 μg/ml), in 0.5 ml sterile solution with 2% (w/v) CMC-Na was injected into the pre-formed air-pouches of mice for immunization with or without 16D10 (1 mM). 16D10 (1 mM) in 0.2 ml of saline was injected every other day for 2 weeks. OVA-specific IgG and IgE in the serum collected 2 weeks after OVA immunization were quantified by ELISA. (C) Diagrammatic representation of the OVA-induced air pouch type allergy model under single application of 16D10. (D) OVA (200 μg/ml), in 0.5 ml sterile solution with 2% (w/v) CMC-Na was injected into the pre-formed air-pouches of mice for immunization with or without 16D10 (1 mM). OVA-specific IgG and IgE in the serum collected 2 weeks after OVA immunization were quantified by ELISA. Data are represented as means ± S.E.M. (n=6-7). $*P < 0.05$ vs. OVA-immunization alone group. N.D.: not detected.

Figure

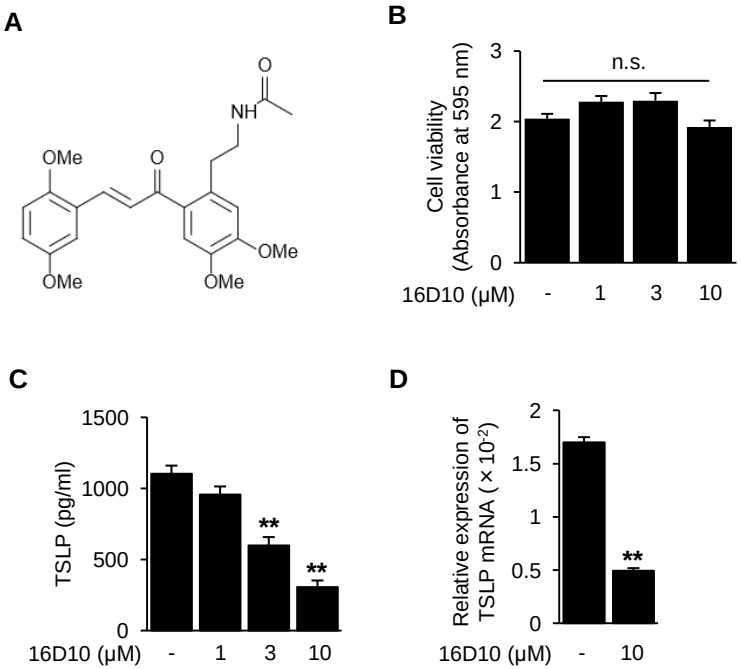
A
O
NH
OMe
O
OMe
OMe
OMe
B
n.s.
Cell viability
(Absorbance at 595 nm)
3
2
1
0
16D10 (μM) - 1 3 10
C
1500
1000
500
0
TSLP (pg/ml)
**
**
16D10 (μM) - 1 3 10
D
2
1.5
1
0.5
0
Relative expression of
TSLP mRNA (× 10-2)
**
16D10 (μM) - 10

**Fig. 1**

**Figure**

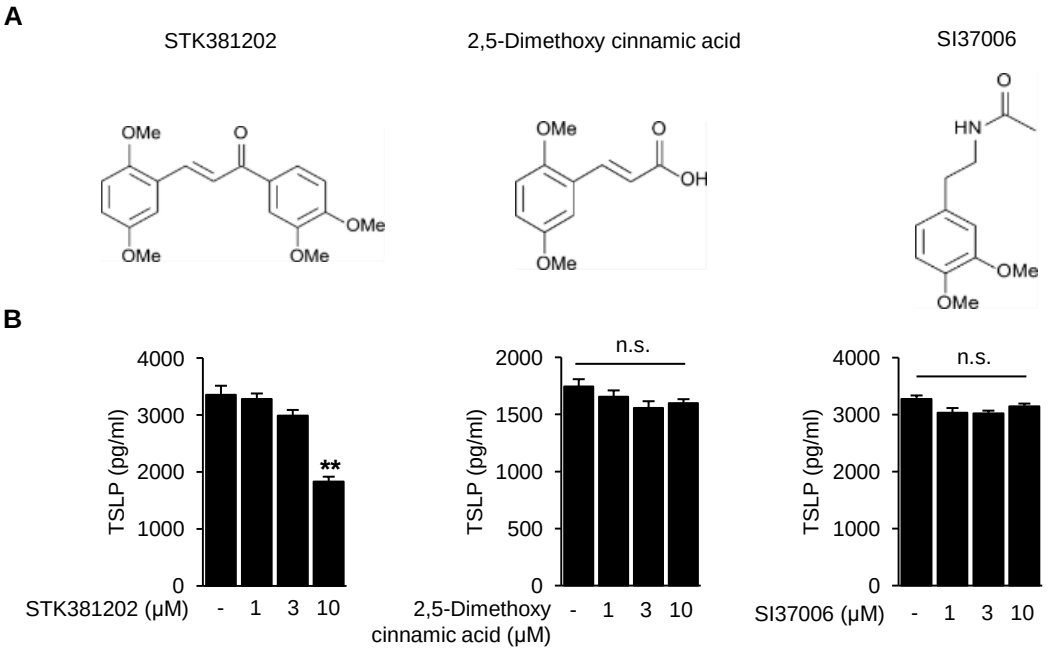
A
STK381202
2,5-Dimethoxy cinnamic acid
SI37006
OMe
O
OMe
OMe
OMe
OMe
OMe
O
OH
OMe
HN
O
OMe
OMe
B
TSLP (pg/ml)
4000
3000
2000
1000
0
**
STK381202 (μM) - 1 3 10
n.s.
2000
1500
1000
500
0
2,5-Dimethoxy cinnamic acid (μM) - 1 3 10
n.s.
SI37006 (μM) - 1 3 10

**Fig. 2**

**Figure**

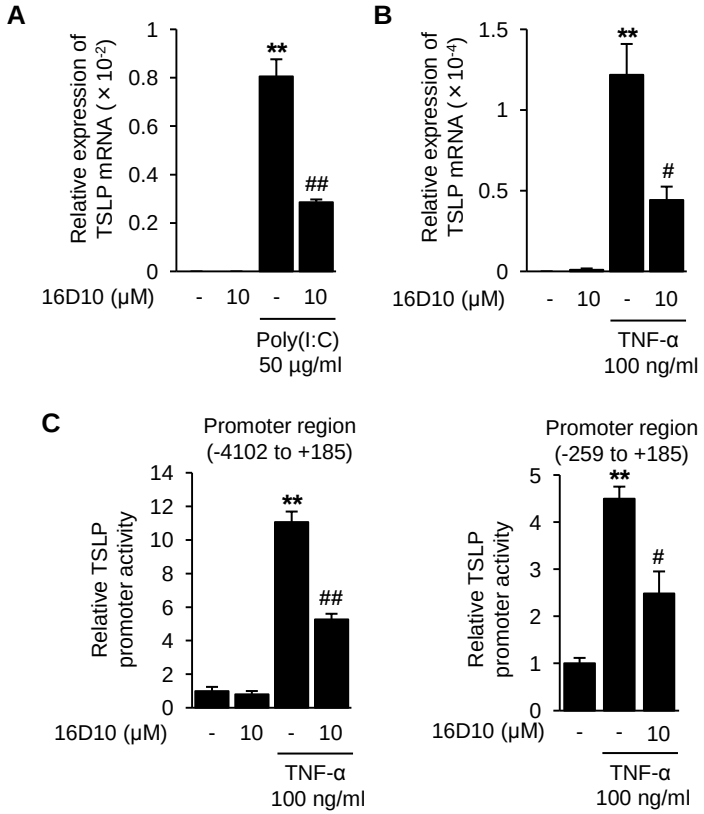
A
Relative expression of TSLP mRNA (×10-2)
1
0.8
0.6
0.4
0.2
0
**
##
16D10 (μM) - 10 - 10
Poly(I:C) 50 μg/ml
B
Relative expression of TSLP mRNA (×10-4)
1.5
1
0.5
0
**
#
16D10 (μM) - 10 - 10
TNF-α 100 ng/ml
C
Promoter region (-4102 to +185)
Relative TSLP promoter activity
14
12
10
8
6
4
2
0
**
##
16D10 (μM) - 10 - 10
TNF-α 100 ng/ml
Promoter region (-259 to +185)
Relative TSLP promoter activity
5
4
3
2
1
0
**
#
16D10 (μM) - - 10
TNF-α 100 ng/ml

**Fig. 3**

Figure

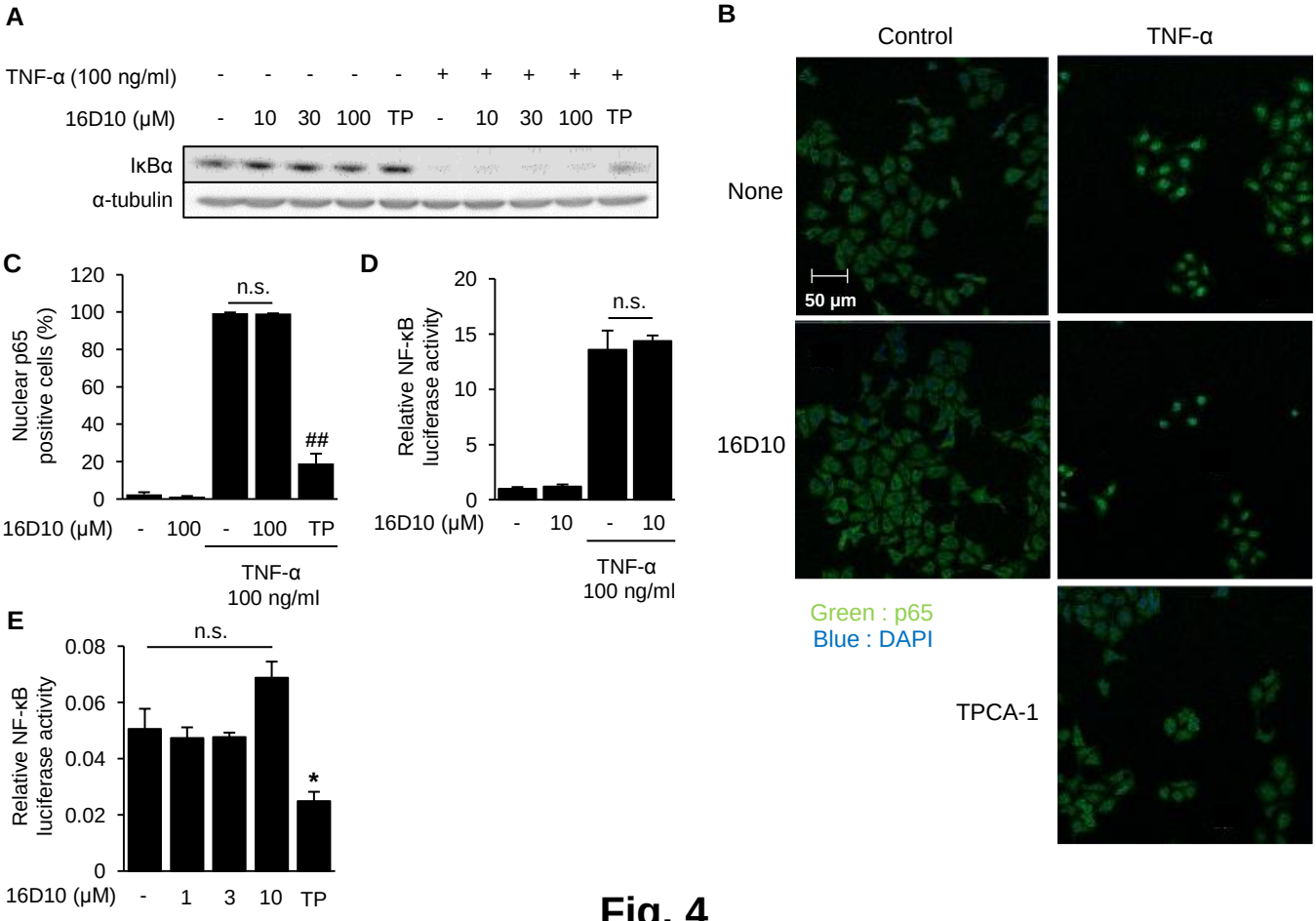
A
TNF-α (100 ng/ml) - - - - - + + + + +
16D10 (μM) - 10 30 100 TP - 10 30 100 TP
IκBα
α-tubulin
B
Control
TNF-α
None
16D10
TPCA-1
50 μm
Green : p65
Blue : DAPI
C
Nuclear p65 positive cells (%)
120
100
80
60
40
20
0
n.s.
##
16D10 (μM) - 100 - 100 TP
TNF-α 100 ng/ml
D
Relative NF-κB luciferase activity
20
15
10
5
0
n.s.
16D10 (μM) - 10 - 10
TNF-α 100 ng/ml
E
Relative NF-κB luciferase activity
0.08
0.06
0.04
0.02
0
n.s.
*
16D10 (μM) - 1 3 10 TP

Fig. 4

Figure

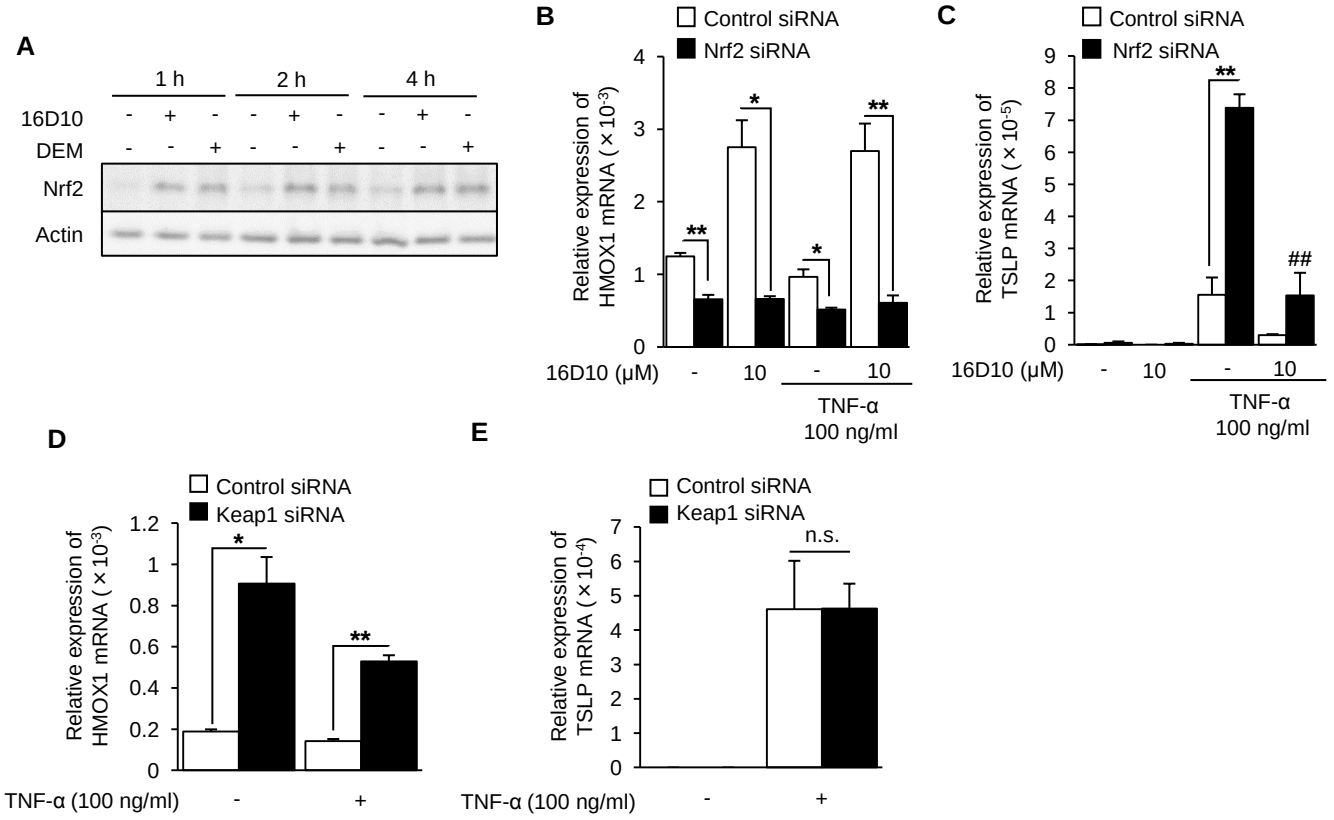
A
1 h
2 h
4 h
16D10
DEM
Nrf2
Actin
B
Control siRNA
Nrf2 siRNA
Relative expression of HMOX1 mRNA (×10-3)
16D10 (μM)
TNF-α 100 ng/ml
C
Control siRNA
Nrf2 siRNA
Relative expression of TSLP mRNA (×10-5)
16D10 (μM)
TNF-α 100 ng/ml
D
Control siRNA
Keap1 siRNA
Relative expression of HMOX1 mRNA (×10-3)
TNF-α (100 ng/ml)
E
Control siRNA
Keap1 siRNA
n.s.
Relative expression of TSLP mRNA (×10-4)
TNF-α (100 ng/ml)

Fig. 5

Figure

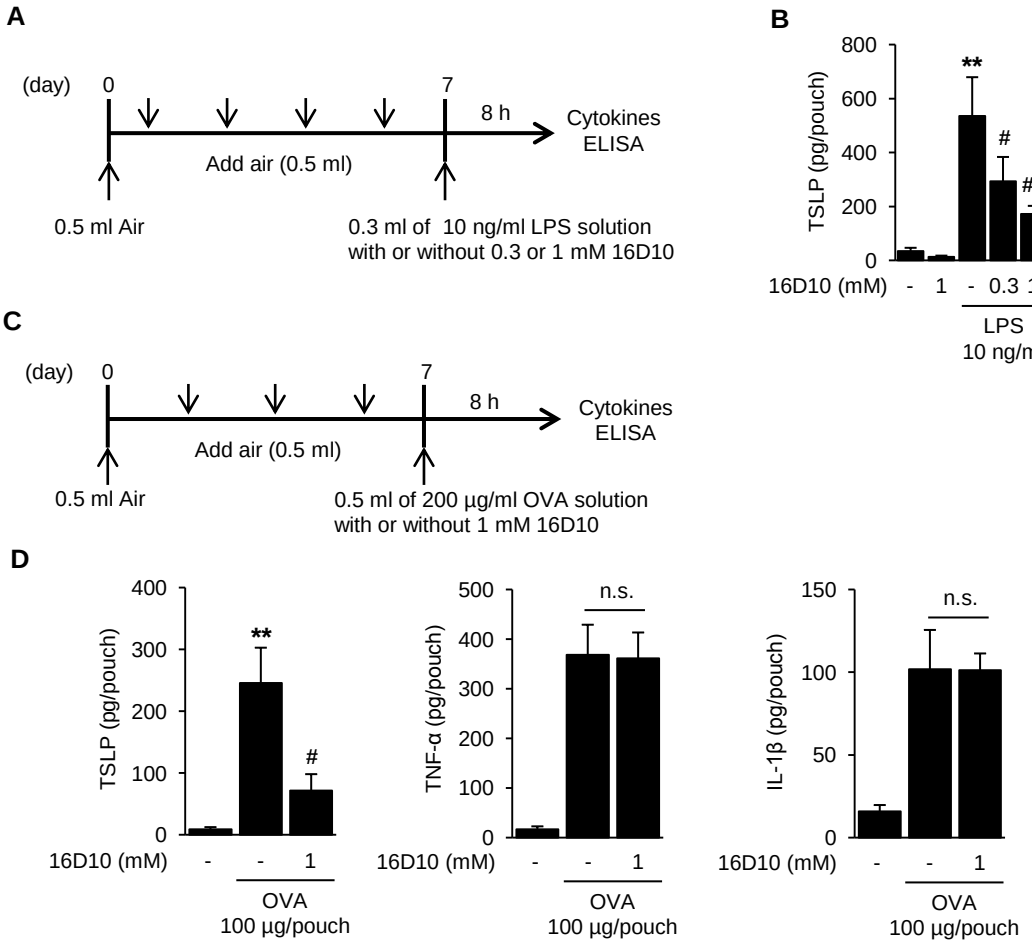
A
(day)
0
7
8 h
Cytokines
ELISA
Add air (0.5 ml)
0.5 ml Air
0.3 ml of 10 ng/ml LPS solution
with or without 0.3 or 1 mM 16D10
B
TSLP (pg/pouch)
800
600
400
200
0
**
#
##
16D10 (mM) - 1 - 0.3 1
LPS
10 ng/ml
C
(day)
0
7
8 h
Cytokines
ELISA
Add air (0.5 ml)
0.5 ml Air
0.5 ml of 200 µg/ml OVA solution
with or without 1 mM 16D10
D
TSLP (pg/pouch)
400
300
200
100
0
**
#
16D10 (mM) - - 1
OVA
100 µg/pouch
TNF-α (pg/pouch)
500
400
300
200
100
0
n.s.
16D10 (mM) - - 1
OVA
100 µg/pouch
IL-1β (pg/pouch)
150
100
50
0
n.s.
16D10 (mM) - - 1
OVA
100 µg/pouch

**Fig. 6**

Figure

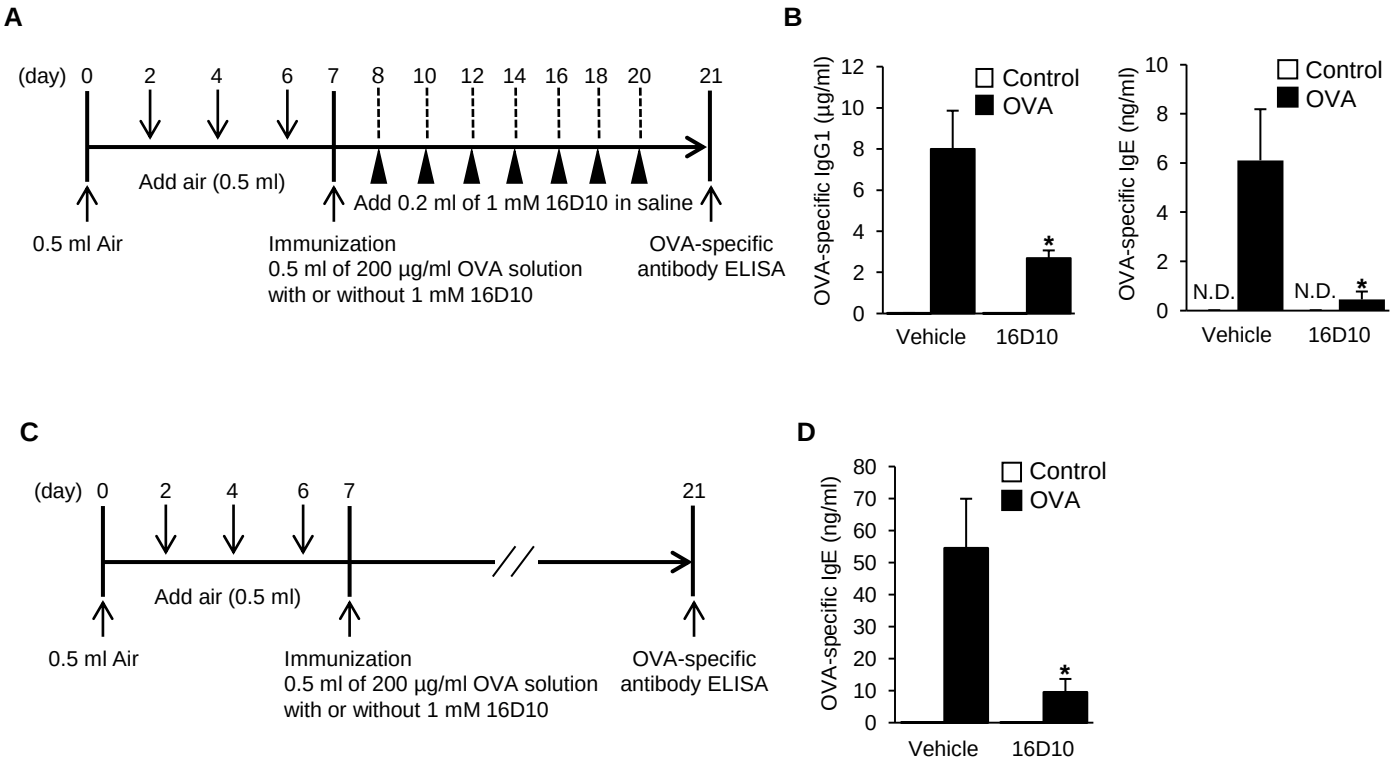
A
(day) 0 2 4 6 7 8 10 12 14 16 18 20 21
Add air (0.5 ml)
Add 0.2 ml of 1 mM 16D10 in saline
0.5 ml Air
Immunization
0.5 ml of 200 µg/ml OVA solution
with or without 1 mM 16D10
OVA-specific
antibody ELISA
B
OVA-specific IgG1 (µg/ml)
Control
OVA
Vehicle
16D10
OVA-specific IgE (ng/ml)
N.D.
N.D.
C
(day) 0 2 4 6 7 21
Add air (0.5 ml)
0.5 ml Air
Immunization
0.5 ml of 200 µg/ml OVA solution
with or without 1 mM 16D10
OVA-specific
antibody ELISA
D
OVA-specific IgE (ng/ml)
Control
OVA
Vehicle
16D10

**Fig. 7**